PREPARATION AND CHARACTERIZATION OF LIGNITE ASHES COATED WITH TiO_2 FOR ENVIRONMENTAL APPLICATION

Eleni Katsika[1], Angeliki Moutsatsou[1], Vayos Karayannis[2], Afroditi Ntziouni[1]

[1] School of Chemical Engineering,
National Technical University of Athens (NTUA)
Zografou Campus, 15773, Athens, Greece
[2] Department of Environmental Engineering
Technological Education Institute
of Western Macedonia, 50100, Kozani, Greece
E-mail: vkarayan62@gmail.com

Received 26 October 2016
Accepted 03 May 2017

ABSTRACT

This research aims at the utilization of both calcareous and siliceous lignite ashes, by-products of lignite combustion in power plants, toward a development of new materials of an environmental benefit. The possibility of fly and bottom ash surface modification by anatase and rutile (titanium dioxide structures) is investigated. The precipitation of TiO_2 from an acidic solution on lignite ash surface is studied and the percentage of TiO_2 coating obtained is found ranging from 11 to 55 %. The latter microstructure is examined by XRD and SEM-EDX taking into consideration the ashes particle size (as received and < 45 μm), the solution pH (5.5 - 7.5), the ageing time (1 and 3 h) and the sintering temperature (300°C, 500°C, 700°C) applied. Anatase and rutile crystalline structures are observed within the whole heat treatment range. The main advantage of the process reported refers to titania immobilization onto a cheap porous substrate providing an additional solution to liquid wastes treatment by photocatalysis.

Keywords: *lignite ashes, titanium dioxide, surface coating.*

INTRODUCTION

The valorization of solid industrial by-products as secondary raw materials in the manufacturing of value-added products can contribute to environmental protection, resources conservation as well as cost reduction [1 - 3]. Besides, current advances in environmental legislation encourage manufacturers to optimize industrial by-products management and utilization. In particular, the valorization of fly ash (FA) and bottom ash (BA) produced in massive quantities from lignite combustion for power generation is nowadays of increasing importance [4 - 6]. The recycling of FA can be a good alternative solution to disposal. It can also provide significant economic and environmental benefits. The global average utilization of FA is estimated to be nearly 25 % of the amount produced [7].

More than 8 million tons of ashes are annually obtained in Greek power stations. Nearly 80 % of the lignite used comes from Northern Greece (West Macedonia) where the main lignite deposits are located. FA is a fine powder obtained by electrostatic precipitation of dust-like particles contained in lignite-fed boilers flue gases. So far, only a small amount of Greek FA is used, while more than 80 % of the overall ash output is directly discharged into ponds and landfills. However, there are concerns that this situation will possibly cause severe and irreversible long-term environmental effects, as FA particles contain toxic trace elements (heavy metals) [8 - 9]. Several studies have already focused upon the addition of FA in clayey mixtures in different combinations and proportions to manufacture

conventional extruded or sintered ceramic materials [1, 3, 10 - 14]. Moreover, various mixtures of several industrial solid wastes containing SiO_2, Al_2O_3 and CaO as predominant oxides have already been utilized for construction applications, including glass-ceramics and cement-based materials [16]. Recent research focuses on the utilization of FA as a synthetic zeolite for remediation of soils contaminated by heavy metals [16]. Also, FA in the form of pellets has been successfully tested as a low cost adsorbent to remove Cu and Cd ions from aqueous solutions [17]. FA can be considered as an attractive raw material in heterogeneous catalysis due to aluminosilicate compounds presence [18, 19]. This is in fact a cost-effective and environmentally friendly method of the waste recycling [20 - 21].

TiO_2 has three crystalline phases in nature - anatase (tetragonal), rutile (tetragonal) and brookite (orthorhombic). Rutile TiO_2 is the most stable form, whereas anatase and brookite are metastable and can be transformed to rutile when heated at a high temperature (~ 750°C). Anatase and rutile TiO_2 are most often reported as photocatalysts, and some research results have recently demonstrated that a mixed form of rutile and anatase TiO_2 displays enhanced photocatalytic ability as the transfer of electrons from anatase to a lower-energy rutile electron-trapping site in the mixed phase could decrease the combination rate of charge carriers in anatase TiO_2 and effectively create catalytic "hot spots" [22].

TiO_2 is the most appropriate semiconductor in photocatalytic oxidation with significant advantages and excellent physicochemical and photocatalytic properties in comparison to the other semiconductors [23]. Inorganic by-products like blast furnace ash as well as the ash of agricultural products have been studied as photocatalysts substrates. The techniques used for TiO_2deposition on the surface of these materials refer to co-grinding at high temperatures [24], sol-gel precipitation [25], thermal spraying, pulsed power deposition, etc.

The current research focuses on the precipitation of TiO_2 on the surface of siliceous and high calcium lignite ash (fly and bottom ash). The products structure is studied following the effect of the parameters of TiO_2 precipitation process and that of the ashes physicochemical characteristics. The research aims to extend the field of ashes application to further treatment of liquid wastes such as dye-house effluents, electroplating, etc. as lignite ashes can adsorb heavy and toxic metals.

EXPERIMENTAL

The highly-calcareous fly ash (FAAD) (Class-C according to ASTM C 618) was obtained from the electrostatic precipitators of the Agios Dimitrios lignite power plant situated in Northern Greece (West Macedo-

Table 1. Chemical analysis of FAAD, BAAD, FAM and BAM.

(%)	SiO_2	Al_2O_3	Fe_2O_3	CaO	MgO	SO_3	Na_2O	K_2O	LoI	
FAAD	30.16	14.93	5.10	34.99	2.69	6.28	1.01	0.40	3.95	*CaOf: 10.87%
BAAD	48.63	21.62	7.29	6.83	2.75	2.78	0.89	2.97	5.34	
FAM	49.54	19.25	8.44	11.82	2.27	3.91	0.53	1.81	2.10	
BAM	50.23	20.40	9.35	7.90	2.30	1.89	0.45	1.98	5.78	*CaOf: 5.95 %

Table 2. Physicochemical characteristics of ashes.

	pH	Particle size distribution (μm)		Specific mass (g/cm^3)
		D(v, 0.5)	D(v, 0.9)	
FAAD	12.5	30.92	98.28	2.67
BAAD	8.5	85.93	199.08	2.74
FAM	11.8	98.92	199.87	2.62
BAM	8.9	97.92	208.14	2.73

Table 3. % TiO_2 precipitated on ashes surface.

	FAAD	BAAD	FAM	BAM
As received	20,13%	55,97%	31,08%	40,94%
< 45 μm	11,37%	20,13%	16,8%	11,22%

Table 4. Characteristics of FAAD and FAM.

Characteristics	FAAD	FAM
Mean Pore Diameter (Å)	160,2	165,1
Pore Volume (cm^3/g)	0,016	0,016

nia, where the main lignite deposits of the country are located). Megalopolis fly ash (FAM), strongly siliceous because of the high SiO_2 content and Ca-bearing species presence, was treated as a Class-C ash. Bottom Ash of Agios Dimitrios and Megalopoli (BAAD and BAM) was a granular material much coarser than FA. It formed during lignite firing and was removed from dry boilers bottom.

The chemical composition of all ashes used was evaluated by X-ray fluorescence (XRF, X-Lab 2000 EDAX, Siemens D-500) and loss on ignition (ASTM D7348). The values of pH were followed in correspondence with ISO 6588, while those of free CaO – with CaOf-ASTM C151. The mineralogical analysis was performed by X-ray Diffraction (Siemens D-500), while the ashes particle size distribution was determined using Malvern MasterSize-S by applying the wet dispersion method.

The physicochemical characteristics and the mineralogical analysis of the ashes studied are given in Tables 1 and 2 as well as in Fig. 1, respectively.

Gypsum ($CaSO_4.2H_20$), quartz (SiO2), lime (CaO), calsite ($CaCO_3$) and a-hematite (Fe_2O_3) were the main crystalline phases of FAAD and BAD. Quartz (SiO_2), silicon oxide (SiO_2), periclasse (MgO) and iron oxide (Fe_2O_3) were the main mineralogical phases for FAM and BAM.

The technique of hydrolysis and simple precipitation was used for coating of lignite ashes surface with TiO_2. This procedure was chosen taking into consideration the physicochemical characteristics of the ashes and the low cost of the process determined the raw material price. An acidic solution of $TiCl_4$ (molar ratio of $TiCl_4$: HCl = 1 : 2.5) was added to 18 g of lignite ash (particles of a size as received or of a size < 45μm after grinding) under stirring to avoid orthotitanate acid formation. Then 81.5 mL 2M NH_4HCO_3 were added and the precipitate obtained was left for aging within 1h. The product was filtered, dried for 24h and sintered for 2 h. The sintering temperature applied referred to 300°C, 500°C and 700°C.

The microstructure was examined by X-ray diffraction

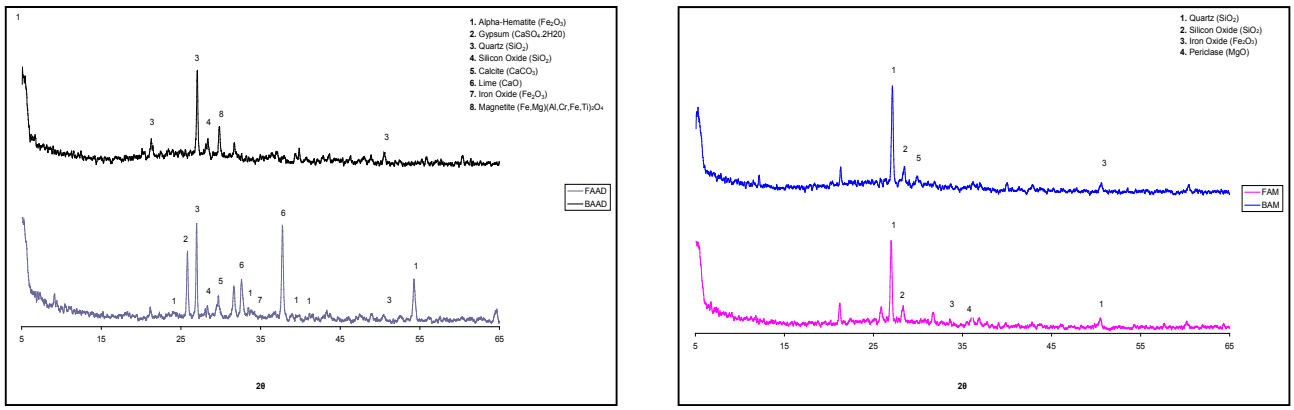

Fig. 1. Minerological analysis of (a) FAAB and BAAD, (b) FAM and BAM.

Table 5. Particle size distribution of coated ashes.

	Particle size (μm)			
	As Received		< 45 μm	
	D(v, 0.5)	D(v, 0.9)	D(v, 0.5)	D(v, 0.9)
FAAD	19,62	76,09	28,88	40,43
BAAD	11,55	224,98	13,64	40,02
FAM	88,82	209,06	15,12	43,46
BAM	77,00	199,60	17,30	47,75

and SEM (FEI Quanta 200 equipped with an EDAX detector).

The adsorption capacity of the material prepared in respect to metal cations was tested in a solution containing Cu^{2+}, Zn^{2+}, $Pb^{2+}$and Cd^{2+} of a various concentration. The optimum results referred to a solution containing 100 ppm of Cu^{2+}, 100 ppm of Zn^{2+}, 5 ppm of Pb^{2+} and 5 ppm of Cd^{2+}. Stirring was applied for 1 h at a rate of 200 rpm.

RESULTS AND DISCUSSION

The percentage of TiO_2 precipitated on the surface of lignite ashes ranges from 11% to 56 % as shown in Table 3. It is worth adding that the process takes place faster at bottom ashes most probably because of their greater porosity. Table 4 illustrates the comparison between FAAD and FAM mean pore diameter and pore volume.

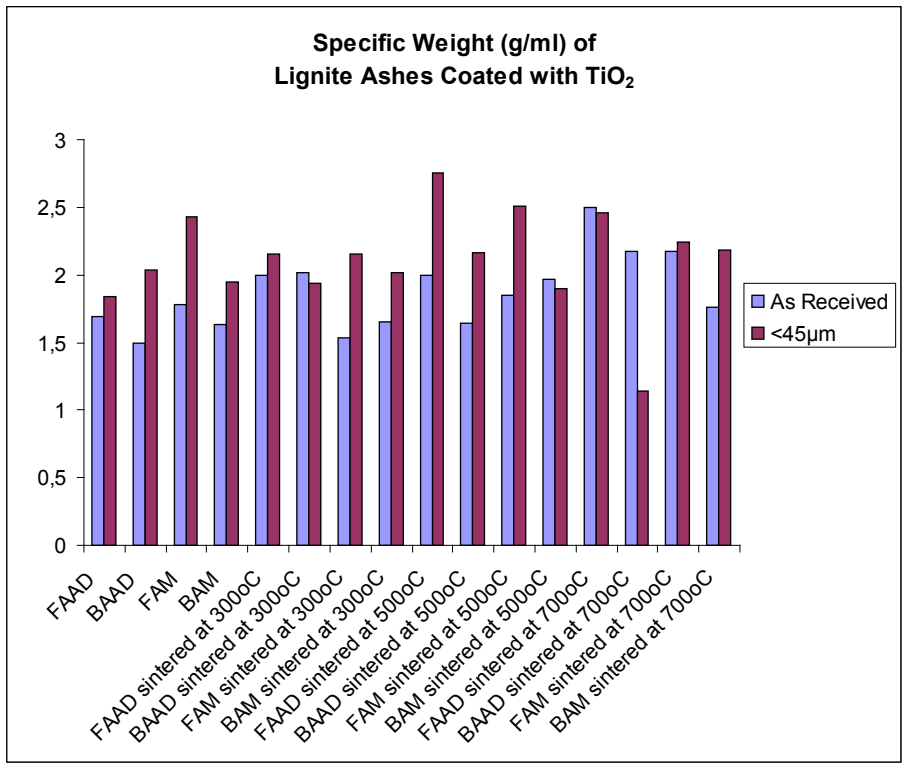

Fig. 2. Specific mass of all products.

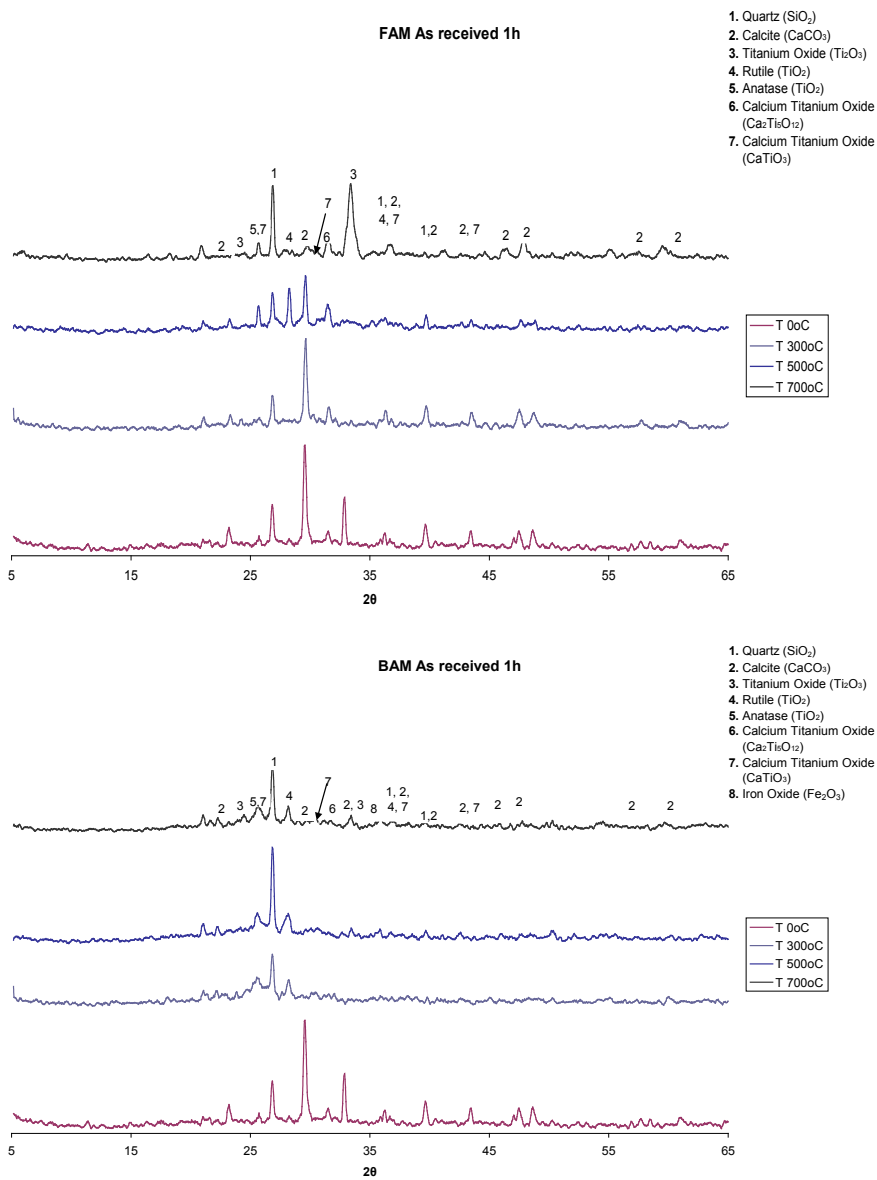

Fig. 3. XRD spectra of green and sintered samples (300°C, 500°C, 700°C - 2 h) (a) coated FAAD; (b) coated BAAD.

The particles' size seems to stays unchanged as shown in Table 5. The specific weight measurements of the specimens illustrated in Fig. 2 cannot lead to yield estimation as the values vary depending on the raw material used.

Fig. 3 presents XRD spectra of green and samples sintered for 2 h at 300°C, 500°C and 700°C. The particle size of the coated FAAD and BAAD samples used refers to that as received, while the ageing time is equal to 1h. It is seen that the crystalline phase of calcite is decomposed upon temperature increase and the phases predominating in the sintered materials refer to quartz (SiO_2), calcium titanium oxide ($CaTiO_3$, $Ca_2Ti_5O_{12}$), anatase and rutile (TiO_2). The coated FAAD sintered at 700°C show a decrease of all phases' content. The presence of TiO_2 is well outlined. This is an undesirable fact in view of the photocatalytic properties expected. The mineralogical examination results provide to conclude that the product sintered at 500°C can be used as a catalyst. Furthermore, it still contains FA phases responsible for heavy metals adsorption [26]. Its adsorption capacity in respect to heavy metals presence is examined using a polymetalic solution. The results obtained are presented in Table 6.

It is well recognized that a mixture of rutile and

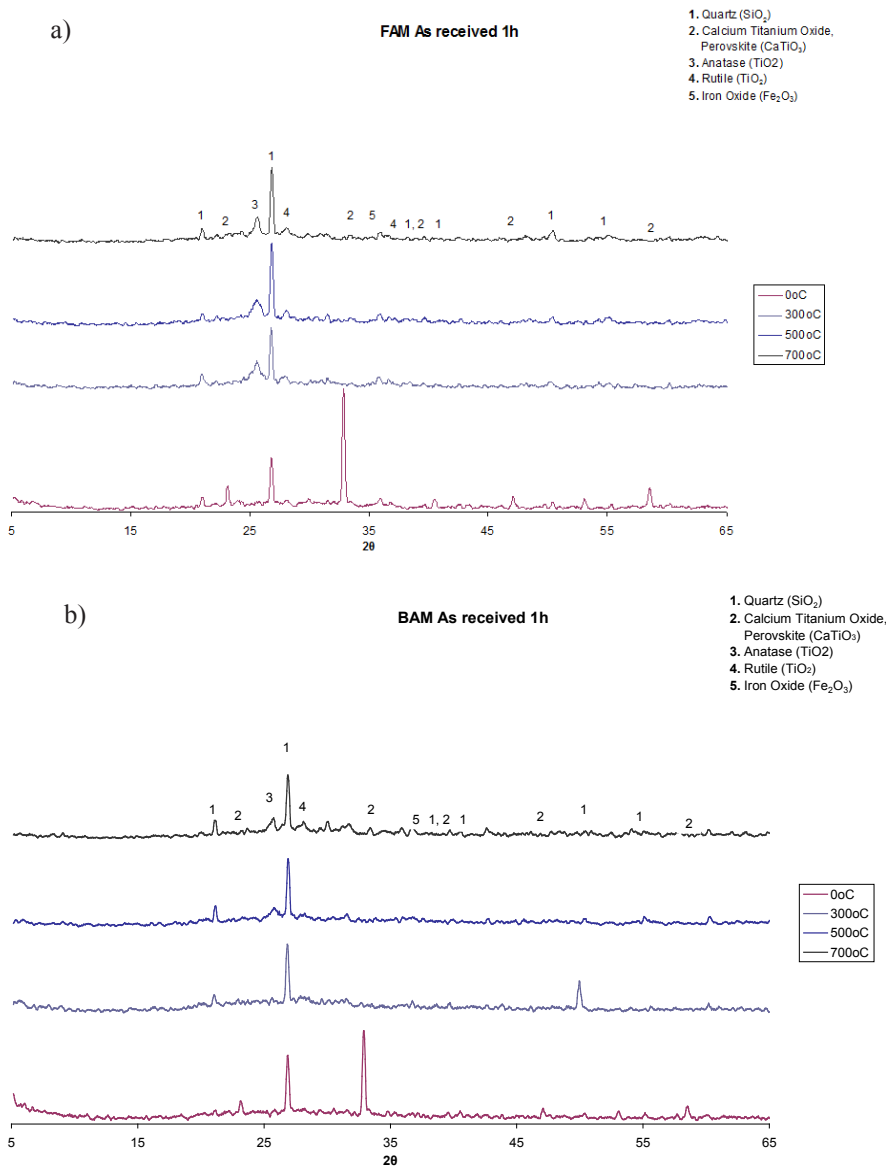

Fig. 4. XRD spectra of green and sintered samples (300°C, 500°C, 700°C - 2 h) of (a) coated FAM; (b) coated BAM.

anatase TiO_2 displays enhanced photocatalytic ability. It is known that the anatase is converted into rutile at temperature > 500°C, but this could be excluded [27-29] due to ashes impurities. Experiments performed with siliceous ashes (FAM, BAM, Fig. 4) show a decomposition of calcium titanium oxide ($CaTiO_3$) with temperature increase. No changes in the mineralogical investigation in relation to the parameters chosen are observed. This fact leads to the conclusion that a quantitative phase determination is required.

The amount of TiO_2 coated on fly ash increases with particle size decrease but without any changes of the mineralogical phases present (Figs. 5, 6). The same behaviour is observed in case of bottom ashes (Figs. 7 and 8).

The rutile percentages are listed in Table 7. The rutile content is estimated on the ground of the X-ray diffraction patterns of the calcinated powder recorded in the diffraction angle range of $2\Theta = 20^O - 80^O$ using CuK_α radiation. Anatase/rutile percentages are calculated using the Spurr -Myers equation:

$$\%_{Rutile} = \frac{1}{1 + 0{,}8\left[\frac{I_A(101)}{I_R(110)}\right]}$$ [30]:

where I_A is the intensity of anatase (101) peak, while I_R is the intensity of rutile (110) peak.

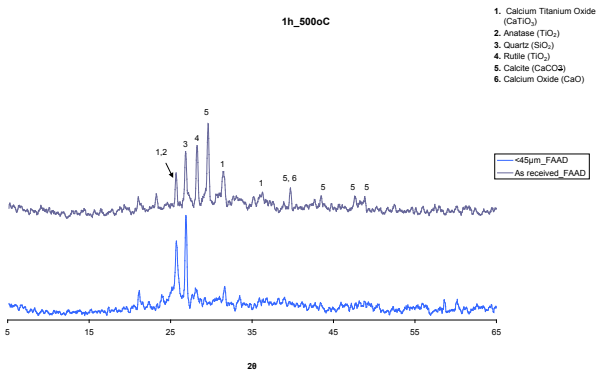

Fig. 5. XRD spectra of coated FAAD sintered samples

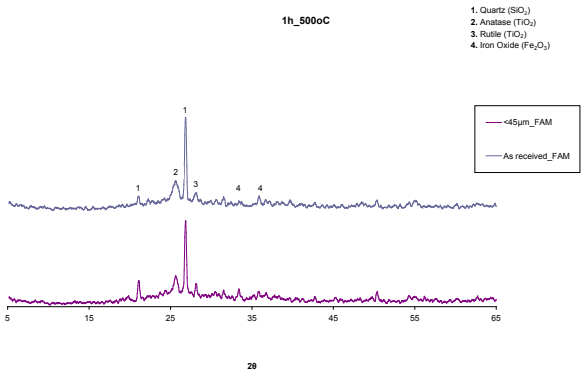

Fig. 6. XRD spectra of (500 °C - 2 h) with different particle size.

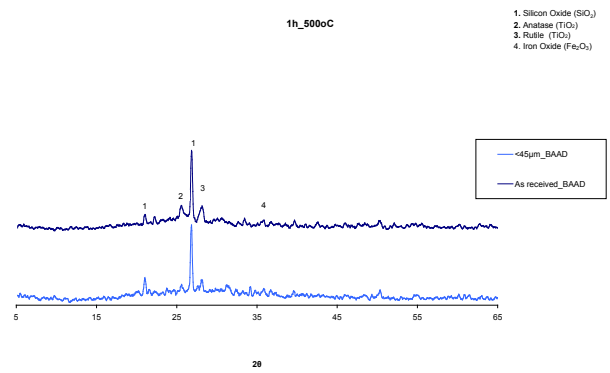

Fig. 7. XRD spectra of sintered (500°C - 2 h) coated BAAD with different particle size.

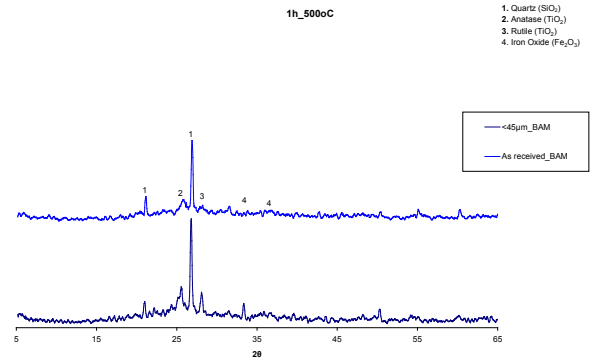

Fig. 8. XRD spectra of sintered (500°C - 2 h) coated BAM, with different particle size.

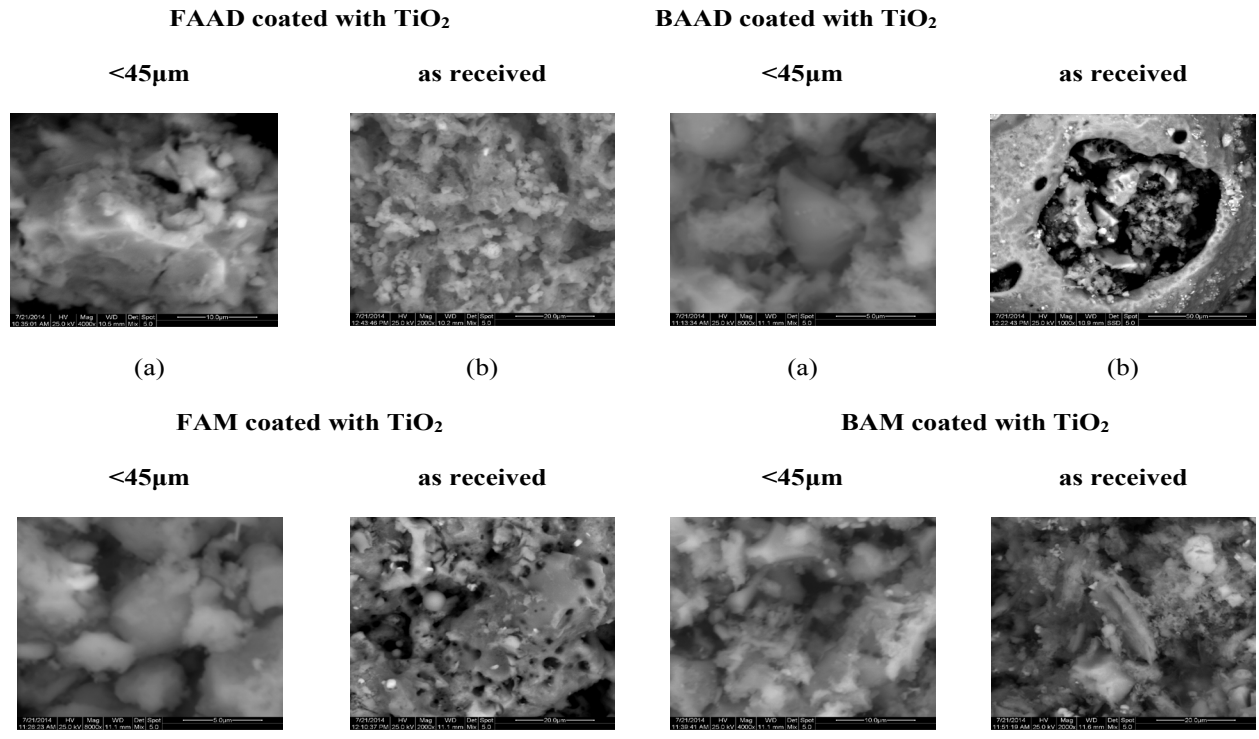

Fig. 9. SEM micrographs of sintered samples (500°C - 2 h) coated FAAD, BAAD, FAM and BAM, with different grain size.

Table 6. Adsorption capacity of coated lignite ashes.

	Cu(mg/g)	Pb(mg/g)	Cd(mg/g)	Zn(mg/g)
FAAD	4,9907	0,2384	0,2407	4,9287
BAAD	4,9863	0,2491	0,2068	4,8022
FAM	4,1600	0,2479	0,2300	4,8076
BAM	3,8504	0,2483	0,0996	4,8152

Table 7. Rutile percentages calculated by Spurr -Myers equation.

	%Rutile	
	As Received	< 45 μm
FAAD (coated with TiO_2) sintered in 500°C	63	32
BAAD (coated with TiO_2) sintered in 500°C	55	54
FAM (coated with TiO_2) sintered in 500°C	44	47
BAM (coated with TiO_2) sintered in 500°C	43	52

The weight fraction of each crystal phase in all TiO_2 powders tested is calculated using the areas of anatase (AA) and rutile (AR) peaks at 25.3° (2Θ) (101) and 27.5° (110) (2Θ), respectively. It can be seen that the coating consists of almost identical amounts of both TiO_2 structures.

A red tint colouring of the specimens is observed. It is better expressed in those of Megalopolis. It is due to Fe compounds transformation to Fe_2O_3 as indicated by XRD.

The SEM micrographs illustrated in Fig. 9 show dense microstructures. The differences caused by the mineralogical phases present and the ashes various granules size are also well outlined. The surface of the BAAD and BAM coated with TiO_2 appears slightly more porous compared to that of coated FAAD and FAM most probably because of the carbon burnout during sintering and the coarser particles. Residual porosity may also, to a certain degree, be attributed to another factor. Thus the fly ash used consists of not only a dense solid, but of hollow particles (cenospheres) as well. The latter are expected to be filled by TiO_2. In any case the porosity is of importance to attain weight reduction of the final products as well as to provide liquid waste treatment using bed reactors filled with ashes.

The EDX analyses carried out shows that the TiO_2 coating contains glassy SiO_2. That on cenospheres consists almost entirely of glassy SiO_2. This indicates that Ti has better behavior in Ca absence, with which it otherwise interacts.

CONCLUSIONS

The process of TiO_2 precipitation on high calcareous and siliceous ashes described in this communication extends their use in the field of photocatalysis, which in turn is of importance for wastewaters treatment.

The experimental results show that the presence of CaO_f in the ashes affects the amount of TiO_2 coating as perovskite (calcium titanium oxide) is produced. The

ashes particle size has a slight effect, while a sintering temperature of 500°C provides the predominant presence of anatase and secondarily rutile.

Furthermore, the ashes impurities prevent anatase conversion to rutile at high temperatures, which favors the photocatalytic properties expected.

REFERENCES

1. P. Muñoz, M.P. Morales, V. Letelier, M.A. Mendivil, Fired clay bricks made by adding wastes: Assessment of the impact on physical, mechanical and thermal properties, Construction and Building Materials, 125, 2016, 241-252.
2. C.-A. Drosou, N. Papadopoulos, A. Moutsatsou, Influence of storage in the degradation of soda lime glass containers, J. Chem. Technol. Metall., 50, 4, 2015, 415-422.
3. K. Komnitsas, Potential of geopolymer technology towards green buildings and sustainable cities, Procedia Engineering, 21, 2011, 1023-1032.
4. V.G. Karayannis, A.K. Moutsatsou, E.L. Katsika, Sintering lignite fly and bottom ashes via two-step versus conventional process, Science of Sintering, 48, 3, 2016, 363-370.
5. A. Karamberi, K. Orkopoulos, A. Moutsatsou, Synthesis of glass-ceramics using glass cullet and vitrified industrial by-products, Journal of the European Ceramic Society, 27, 2-3, 2007, 629-636.
6. S. Tsimas, A. Moutsatsou-Tsima, High-calcium fly ash as the fourth constituent in concrete: problems, solutions and perspectives, Cement & Concrete Composites, 27, 2, 2005, 231-237.
7. Z.T. Yao, X.S. Ji, P.K. Sarker, J.H. Tang, L.Q. Ge, M.S. Xia, Y.Q. Xi, A comprehensive review on the application of coal fly ash, Earth-Science Reviews, 141, 2015, 105-121.
8. M.M. Pergal, D. Relić, Ž.L. Tešić, A.R. Popović, Leaching of polycyclic aromatic hydrocarbons from power plant lignite ash-influence of parameters important for environmental pollution, Environmental Science and Pollution Research, 21, 5, 2014, 3435-3442.
9. V. Tsiridis, M. Petala, P. Samaras, A. Kungolos, G.P. Sakellaropoulos, environmental hazard assessment of coal fly ashes using leaching and ecotoxicity tests, Ecotoxicology and Environmental Safety, 84, 2012, 212-220.
10. V.G. Karayannis, A.K. Moutsatsou, E.L. Katsika, Synthesis of microwave-sintered ceramics from lignite fly and bottom ashes, Journal of Ceramic Processing Research, 14, 1, 2013, 45-50.
11. B. Kim, M. Prezzi, Compaction characteristics and corrosivity of Indiana class-F fly and bottom ash mixtures, Construction & Building Materials, 22, 2008, 694-702.
12. V. Adell, C.R. Cheeseman, A. Doel, A. Beattie, A.R. Boccaccini, Comparison of rapid and slow sintered pulverised fuel ash, Fuel, 87, 2, 2008, 187-195.
13. J.C. Hower, Characterization of fly ash from Kentucky power plants, Fuel and Energy Abstracts, 37, 3, 1996, 184.
14. A. Jonkera, J.H. Potgieter, An evaluation of selected waste resources for utilization in ceramic materials applications, Journal of the European Ceramic Society, 25, 2005, 3145-3149.
15. A. Karamberi, A. Moutsatsou, Vitrification of lignite fly ash and metal slags for the production of glass and glass ceramics, China particuology, 4, 5, 2006, 250-253.
16. A. Moutsatsou, V. Protonotarios, Remediation of polluted soils by utilizing hydrothermally treated calcareous fly ashes, China Particuology, 4, 2, 2006, 65-69.
17. A. Papandreou, C.J. Stournaras, D. Panias, Copper and cadmium adsorption on pellets made from fired coal fly ash, J. Hazard. Mater., 148, 2007, 538-547.
18. A. Farook, J. N. Appaturi, R. Thankappan, M. Asri, M. Nawi, Silica–tin nanotubes prepared from rice husk ash by sol–gel method: Characterization and its photocatalytic activity, Original Research Article Applied Surface Science, 2010, 257, 811-816.
19. C.F. Wang, J.S. Li, L.J. Wang, X.Y. Sun, Influence of NaOH concentrations on synthesis of pure-form zeolite A from fly ash using two-stage method, J. Hazard. Mater. 15558,2008, 64.
20. S. Wang, Application of solid ash based catalysts in heterogenous catalysis, Environ. Sci. Technol., 42, 2008, 7055-7063.
21. Yan Wang, Yiming He, Qinghua Lai, Maohong Fan, Review of the progress in preparing nano TiO_2: An important environmental engineering material, Journal Of Environmental Sciense, 26, 2014, 2139-2177
22. A. Katsanaki, Photocatalytic activity of nanostructured titanium oxide materials in standardized reac-

tors of air pollutants. PhD Thesis, National Technical Univ. of Athens, Greece, 2012.
23. X. Lei, X. Xue, Preparation, characterization and photocatalytic activity of sulfuric acid-modified titanium-bearing blast furnace slag, Transactions of Nonferrous Metals Society of China, 20, 12, 2010, 2294-2298.
24. J.-W. Shi, S.-H. Chen, S.-M. Wang, P. Wu, G.-H. Xu, Favorable recycling photocatalyst TiO_2/CFA: Effects of loading method on the structural property and photocatalytic activity, Journal of Molecular Catalysis A: Chemical, 303, 1-2, 2009, 141-147.
25. F. Adam, J.N. Appaturi, R. Thankappan, M.A.M. Nawi, Silica–tin nanotubes prepared from rice husk ash by sol–gel method: Characterization and its photocatalytic activity, Applied Surface Science, 257, 2010, 811-816.
26. M. Visa, R.A. Carcel, L. Andronic, A. Duta, Advanced treatment of wastewater with methyl-orange and heavy metals on TiO_2, fly ash and their rmixtures, J.Catal. Today, 144, 2009, 137–142.
27. Jeong Hoon Lee, Yeong Seok Yang, Effect of hydrolysis conditions on morphology and phase content in the crystalline TiO_2 nanoparticles synthesized from aqueous $TiCl_4$ solution by precipitation, Materials Chemistry and Physics, 93, 1, 2007, 237-242
28. Jeong Hoon Lee, Yeong Seok Yang, Effect of HCl concentration and reaction time on the change in the crystalline state of TiO_2 prepared from aqueous $TiCl_4$ solution by precipitation, Journal of the European Ceramic Society, 25, 16, 2005, 3573-3578.
29. Jian-wen Shi, Shao-hua Chen, Shu-mei Wang, Peng Wu, Gui-hua Xu, Favorable recycling photocatalyst TiO_2/CFA: Effects of loading method on the structural property and photocatalytic activity, Journal of Molecular Catalysis A: Chemical 303, 1-2, 2009,141-147.
30. R. Spurr, H. Myers, Quantitive Analysis of Anatase-Rutile Mixures with an X-Ray Diffractometer, Anal. Chem., 29, 1996, 760.